Evidence for Localized Cell Heating Induced by Infrared Optical Tweezers

Y. Liu,* D. K. Cheng,* G. J. Sonek,* M. W. Berns,‡ C. F. Chapman,‡ and B. J. Tromberg‡
*Department of Electrical and Computer Engineering and Beckman Laser Institute and Medical Clinic, University of California, Irvine, and ‡Department of Biophysics, and Beckman Laser Institute and Medical Clinic, University of California, Irvine, California 92717 USA

ABSTRACT The confinement of liposomes and Chinese hamster ovary (CHO) cells by infrared (IR) optical tweezers is shown to result in sample heating and temperature increases by several degrees centigrade, as measured by a noninvasive, spatially resolved fluorescence detection technique. For micron-sized spherical liposome vesicles having bilayer membranes composed of the phospholipid 1,2-diacyl-pentadecanoyl-glycero-phosphocholine (15-OPC), a temperature rise of $\sim 1.45 \pm 0.15$°C/100 mW is observed when the vesicles are held stationary with a 1.064 μm optical tweezers having a power density of $\sim 10^7$ W/cm^2 and a focused spot size of ~0.8 μm. The increase in sample temperature is found to scale linearly with applied optical power in the 40 to 250 mW range. Under the same trapping conditions, CHO cells exhibit an average temperature rise of nearly 1.15 ± 0.25°C/100 mW. The extent of cell heating induced by infrared tweezers confinement can be described by a heat conduction model that accounts for the absorption of infrared (IR) laser radiation in the aqueous cell core and membrane regions, respectively. The observed results are relevant to the assessment of the noninvasive nature of infrared trapping beams in micromanipulation applications and cell physiological studies.

INTRODUCTION

Since Ashkin et al. (1986) first described the optical trapping of micrometer-sized dielectric particles in a single beam gradient force trap, optical laser traps (optical tweezers) have been successfully used in a variety of biological applications (Kuo and Sheetz, 1992; Svoboda and Block, 1994; Schutze and Clement-Sengewald, 1994) including, for example, the trapping of viruses, bacteria, cells, and organelles (Ashkin and Dziedzic, 1987, 1989; Ashkin et al., 1987), the micromanipulation of gametes (Tadir et al., 1989; Colon et al., 1992; Schutze et al., 1994), the study of chromosome movement (Berns et al., 1989; Vorobjev et al., 1993; Liang et al., 1994), the tensiometric measurement of motor protein molecules (Block et al., 1990; Kuo and Sheetz, 1993; Svoboda et al., 1993; Finer et al., 1994), and the study of DNA molecule physics (Perkins et al., 1994). Some of these studies indicated that, due to lower chromophore absorption at the longer laser wavelengths, the Nd:YAG laser wavelength (1.064 μm) was more effective in trapping various cells and subcellular organelles without inducing apparent cell damage. The present work attempts to quantify the extent of cell heating at this wavelength, as part of a larger effort to relate induced thermal effects to observed variations in cell physiology as a result of trapping. The relative importance of thermal effects in optical traps and their direct and indirect impact on motile and non-motile cell function and behavior should be assessed, given the extensive use of optical tweezers in biological studies at the cellular and molecular levels. We provide experimental evidence for localized sample heating induced by infrared optical tweezers.

We previously reported on a microfluorometric technique for making thermal measurements with micron spatial resolution (Liu et al., 1994), based on the optical measurement of temperature-dependent fluorescence spectra from dye-labeled bilayers (Parasassi et al., 1990, 1991) in liposomes (Oku et al., 1982; Yatvin et al., 1987). In this paper, we report on the application of this technique to the measurement of temperature changes in single living cells confined by an infrared optical tweezers. We assess the extent of localized heating produced by a Nd:YAG trapping laser beam when it is focused to its near-diffraction-limited spot size. In a confocal microscope geometry, a microscope objective (1.3 N.A., 100×) is used to couple an infrared trapping beam (1.064 μm) and a collinear ultraviolet (UV) excitation beam (365 nm) onto a sample. While the IR beam creates a gradient force trap which confines the single cell sample, the UV beam excites fluorescence from the liposome or cell membrane region, which has been labeled with an environmentally and temperature-sensitive Laurdan (6-dodecanoyl-2-dimethyl aminonaphthalene) dye probe. The sample is assumed to consist of an aqueous core, surrounded by a thin (~5 nm) phospholipid bilayer membrane which contains the dye probe. With the absorption of infrared radiation from the trapping beam by the cell core and membrane regions, the sample becomes heated and, at a specific transition temperature, the bilayer membrane of the sample undergoes a phase transition from a gel to a liquid crystalline state, with a corresponding change in the membrane permeability to water. This transition is accompanied by a large Stokes shift in the probe fluorescence emission spectrum. The emission from micron-sized regions of the membrane is then collected by the same focusing objective and used to directly quantify the change in localized temperature with fluorescence emission shifts as a function of applied laser trapping power or wavelength. These same measurement techniques can also be used

Received for publication 14 September 1994 and in final form 31 January 1995.

Address reprint requests to Dr. Gregory J. Sonek, Department of Electrical and Computer Engineering, University of California, Irvine, CA 92717. Tel.: 714-824-6421-; Fax: 714-824-3732; E-mail: gjsonek@uci.edu.

0006-3495/95/05/2137/08 $2.00

to map the thermal profiles of optically trapped biological samples with high spatial and thermal resolution.

MATERIALS AND METHODS

Sample preparation

Liposome vesicles were prepared (Oku et al., 1982) by mixing the phospholipid 1,2-diacyl-pentadecanoyl-glycero-phosphocholine (15-OPC) (Avanti Polar Lipids, Alabaster, AL) with the dye probe Laurdan (6-dodecanoyl-2-dimethylaminonaphthalene) (Molecular Probes, Eugene, OR) in molar ratios of between 100:1 and 1000:1 in a 200-ml flask containing a chloroform solution. The solution was then dried in a rotary evaporator under vacuum. Subsequently, water-saturated nitrogen was passed through the flask for 20 min. To produce large unilamellar vesicles, the dried lipids were first immersed in a 0.2 M sucrose solution for 2 h at 47°C and then centrifuged at 12,000 *g* for 10 min. Multilamellar vesicles were produced by resuspending the dried lipid samples in a phosphate-buffered saline (PBS) solution (catalog no. D1408, Sigma, St. Louis, MO), heating the mixture to 55°C, and then vortexing the solution. The unilamellar and multilamellar structures of the vesicle membranes for these two sample types were confirmed using scanning electron microscopy (SEM) (model SEM 515, Phillips, Eindhoven, The Netherlands). Since Laurdan is an amphiphilic molecule, it is automatically incorporated into the membrane of the liposome during the phospholipid molecule aggregration process (Fig. 1). These procedures produced nearly spherical Laurdan-labeled liposomes that could vary in size from ~0.1 to 20 μm in diameter.

In the preparation of living cells, Chinese hamster ovary (CHO) cells were maintained in culture using standard procedures (Freshney, 1987). For suspension measurements, the cells were labeled while attached in 25 cm^2 tissue culture flasks. A 4×10^{-4} M solution of Laurdan in ethanol was added to the cell-containing medium such that the ethanol concentration was 3%. The medium itself consisted of GIBCO's minimum essential medium, supplemented with 10%/v fetal bovine serum, 2 mM L-glutamine, 100 U/ml penicillin, and 100 mg/ml streptomycin (all chemicals from Life Technologies, Inc., Grand Island, NY). The cells were first incubated at 37°C for 35 min, and then treated with 0.25% trypsin to cause the cells to detach, followed by a fresh medium rinse to deactivate the enzyme. The medium with detached cells was placed in a culture tube and centrifuged for 5 min at 1000 *g*. The supernatant was removed and the cell pellets were then resuspended in PBS. This procedure resulted in dye-tagged CHO cells having typical sizes of ~8–15 μm in diameter.

Optical trapping and fluorescence spectroscopy

An experimental system was developed for the simultaneous implementation of optical trapping and fluorescence spectroscopy (Fig. 2). An optical

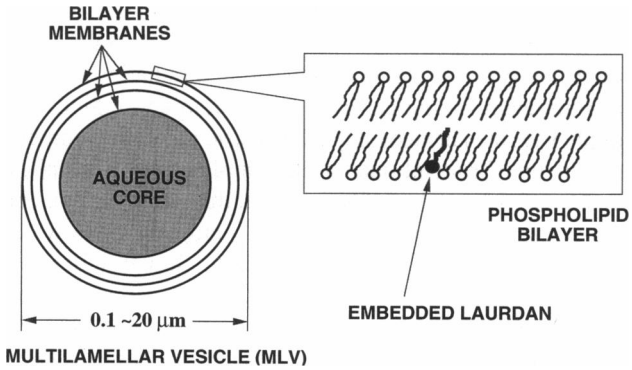

FIGURE 1 Structure of a multilamellar liposome vesicle, consisting of a phospholipid bilayer. A Laurdan dye probe is embedded within the bilayer membrane and used to sense localized temperature changes.

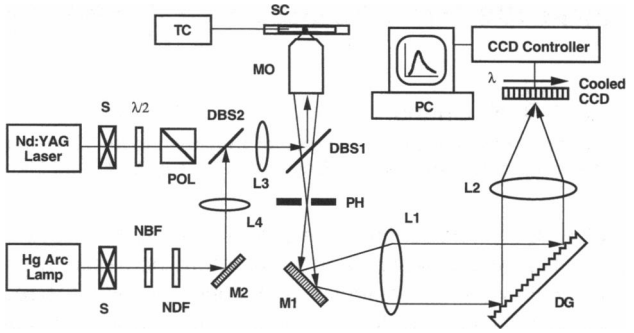

FIGURE 2 Experimental system for implementing fluorescence excitation and detection within an optical tweezers. System components are: Nd:YAG laser; Hg Arc lamp; S: shutter; λ/2: half-wave plate; POL: polarizer; NBF: narrow band filter; NDF: neutral density filter; DBS: dichroic beam splitter; L: lens; MO: microscope objective; SC: sample chamber; TC: temperature controller; PH: pinhole aperture; M: mirror; DG: diffraction grating; CCD: charge-coupled detector; and PC: personal computer. A UV excitation beam is first made collinear with an IR trapping laser beam. Both beams are then focused onto the sample via a high magnification, large numerical aperture objective. This same objective lens collects sample fluorescence and directs the light through a customized spectrometer for signal spectral analysis. A pinhole turns the setup into a confocal tweezers system.

trapping beam was derived from a Nd:YAG laser (model 114, Quantronix, Smithtown, NY) that could emit up to 1 W CW in the TEM_{00} mode at a wavelength of 1.064 μm. Upon emerging from the laser, the polarization of the IR beam is set using an IR polarizer (model 05BC16-PC.9, Newport/Klinger, Irvine, CA). The beam is then directed into a high magnification (×100) and large numerical aperture (1.3 N.A.) oil immersion microscope objective (Zeiss Neofluar) to form the basic optical trap. A 365-nm UV excitation beam is derived from a 200 W Hg arc lamp (model 66006, Oriel, Stamford, CT) that is used in conjunction with a narrow-band filter (model F10–365, CVI, Livermore, CA) having a center wavelength of 365 nm and a band width of 4 nm. This beam is made collinear with the IR trapping beam and then deflected into the focusing objective via a UV/IR dichroic beam splitter (Newport/Klinger model 20SM20HB.14). An electronic shutter (Uniblitz VS14 Shutter and T132 Driver, Vincent Assoc., Rochester, NY) is used to control the fluorescence excitation time. A UV exposure time of 100 ms was used for all experiments and was found to be short enough to prevent photobleaching of the Laurdan dye. The fluorescence emission from the optically trapped sample is collected by the same objective lens and passed through an adjustable pinhole located at the image plane of the microscope objective. A 0.1-to 1-mm diameter pinhole effectively converts the optical system into a confocal trapping microscope that has micron spatial resolution. A 300 g/mm diffraction grating (model 510–18–050, Instruments SA, Edison, NJ) is then used to disperse the light, which is subsequently focused onto an electrically cooled CCD array (model TE/CCD-576E&EM and ST-130 Camera Controller, Princeton Instruments, Trenton, NJ). Spectral data, collected over a 400-nm band width, is acquired and analyzed using a 386 25 MHz NEC personal computer. For sample sizes in the 2- to 20-μm size range, the detected fluorescence signal-to-noise ratio (S/N) was found to exceed 10^3:1.

Temperature sensing and control

A customized sample chamber and temperature control system was constructed for containing the liposome and cell suspensions and controlling the cell solution temperature. The chamber (Fig. 3) consisted of two distinct microchambers placed one on top of the other, created by 170-μm-thick coverslips which formed the outer chamber walls and separated by a thin coverslip in between. The chamber side walls were formed with 3-mm-thick silicone gaskets. The double microchamber design not only served to keep cells sterile but also to maintain a stable sample temperature by minimizing

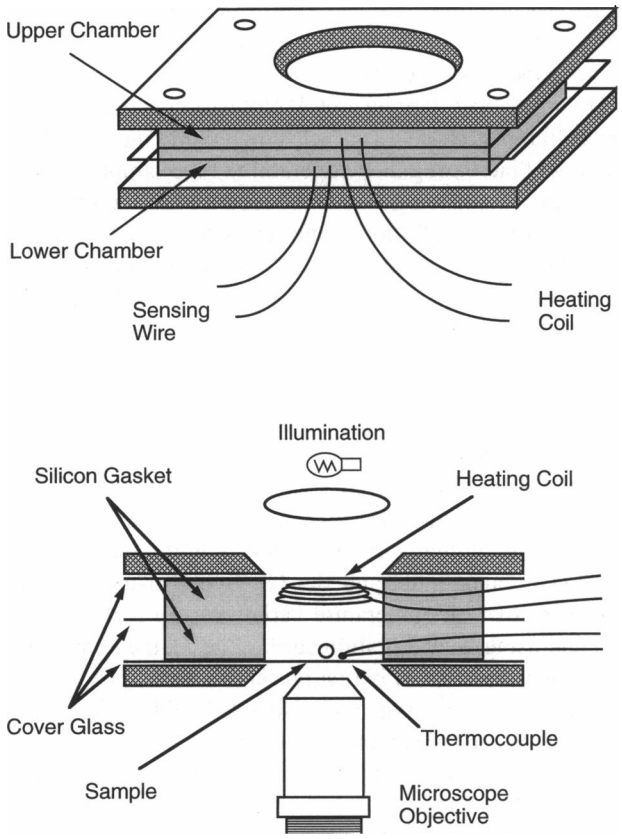

FIGURE 3 Schematic showing the details of the sample chamber and heating system. Two microchambers, separated by an ultrathin glass coverslip, are used to provide direct control and monitoring of the solution and sample temperature in the vicinity of the laser tweezers focal position.

the effects of fluid turbulence in the upper microchamber during the heating process. In the upper microchamber, which was filled with deionized water, an electrically controlled heating coil was introduced through the silicone gasket for the purpose of heating up the fluid medium. This heat is then conducted to the lower microchamber through a glass coverslip which partitions the upper and lower microchambers. In the lower microchamber, a thermocouple (model CHCO-003, Omega Engineering, Stamford, CT) was placed at the center of the chamber to monitor the background solvent solution temperature. The tip of the thermocouple was placed against the surface of the bottom coverslip and very close to the location (within 20–100 μm) of the liposome or cell under study. This technique minimized calibration errors that might result due to the existence of temperature gradients inside the microchambers. By controlling the heating coil current supplied by a power supply (model 6236B, Hewlett-Packard, Palo Alto, CA), the temperature at the bottom of the lower microchamber could be controlled from room temperature (20°C) up to ~60°C, with an accuracy of ±0.03°C. With a customized electronic feedback circuit, this geometry was used to adjust and maintain a set point temperature for a liposome or cell and, at the same time, provide clear optical access for trapping, illumination, and fluorescence excitation beams.

Calibration of laser trapping power

The measurement and calibration of laser trapping power is critical to the determination of induced heating effects. To determine the amount of power reaching the trapped sample, the IR laser power was calibrated and measured at two locations. First, the amount of power that was actually transmitted by the trapping microscope objective (MO) was calibrated using the dual-objective transmittance measurement technique of Misawa et al. (1991). In this method, two identical MOs are used to focus and recollimate the transmitted beam under the exact coupling conditions in which the MOs are being used experimentally, thereby eliminating the errors that might be encountered from a direct lens-to-photodetector transmission measurement. The beam that is focused by the primary trapping objective was transmitted through immersion oil, a coverslip, a thick (~100 μm) water layer, another coverslip, more immersion oil, and was finally collected by an identical microscope objective (Zeiss Neofluar 100×, 1.3 N.A. phase contrast) and detected by a photodetector (model 210, Coherent, Palo Alto, CA). The second MO recollimates the highly divergent beam emerging from the trapping objective, thereby giving an accurate measurement of the total transmission for the two objectives. The transmission of a single objective lens is then given as the square root of the total transmittance for the dual-objective geometry. The measured transmission for a single objective was found to be 0.60 ± 0.05. This figure is consistent with the previously reported value of 0.59 obtained for the same objective lens (Svoboda and Block, 1994). Second, the incident laser power was continuously monitored directly in front of the microscope objective entrance aperture using a photodetector (Coherent model 210). The power incident on the MO entrance aperture could be continuously adjusted using a combination half-wave plate (Newport/Klinger model 05RP12) and polarizer (Newport/Klinger model 05BC16-PC.9) that was placed in the path of the Nd:YAG laser beam (Fig. 2). The calibrated transmission factor was then used in combination with the incident beam measurement in front of the trapping objective to determine the actual laser power at the beam focus of the optical tweezers, with an accuracy of ± 1 mW. In addition, a measurement of the spot size at the beam focus was also performed (Wright et al., 1994), so that a focused beam power density could be determined. Using the scanning knife-edge technique of Firester et al. (1974), a lithographically defined chromium "knife-edge" was rastered across the plane of the beam focus, using high-resolution piezo-driven stages controlled by a custom piezo-driver, consisting of an electronic DC amplifier, power supply (Hewlett-Packard model 6237B), and pulse function generator (Hewlett-Packard model 8116A). A measurement of the beam intensities at the 10% and 90% points facilitated a measurement of the focused spot size, determined to be ~0.80 ± 0.15 μm for the Zeiss 100× MO.

Generalized polarization measurements

The basis for making localized temperature measurements on optically confined samples is the measurement of Stokes-shifted fluorescence emission as a function of sample temperature, from which generalized polarization (GP) can be derived. GP was first described by Parasassi et al. (1990, 1991) in studies of the relaxation dynamics and temperature sensitivity of Laurdan in phospholipid vesicles. Sample fluorescence emission is first measured (Fig. 2) by acquiring spectral data at different sample temperatures (Fig. 4) and calculating the peak emission wavelength at each temperature. GP is defined as the ratio $(I_g - I_l)/(I_g + I_l)$, where I_g and I_l are the fluorescence intensities measured at the maximum emission wavelengths of the Laurdan dye, when the membrane bilayer, having a thickness of ~5 nm, is in its pure gel and liquid-crystalline states, respectively. We note that the gel state is formed at a temperature that is lower than that of the liquid-crystalline state. As the bilayer transitions between these two states with an increase in temperature, the sample fluorescence emission undergoes a red shift, and the magnitude of GP decreases as I_g decreases and I_l increases. Since this process is reversible, a decrease in sample temperature would correspond to a decrease in I_l, an increase in I_g, and an increase in the magnitude of GP. For the phospholipid 15-OPC tagged with Laurdan, the peak wavelengths corresponding to the pure gel and liquid-crystalline states are 440 nm (26°C) and 490 nm (38°C), respectively (Fig. 4). Given the possibility of dye photobleaching and UV-induced light stress, the intensity and duration of the UV excitation beam was carefully controlled. Under these conditions, S/N ratios of $>10^3$:1 and $>10^2$:1 were achieved for the liposome and CHO samples, respectively.

Error analysis

There are several sources of experimental error that determine the sensitivity of the GP assay used herein and, hence, the smallest change in GP that can

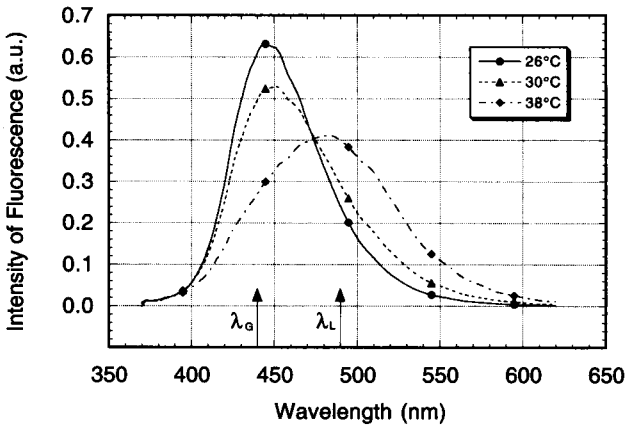

FIGURE 4 Spectral plots showing the Stokes shift in fluorescence emission with increasing temperature for a 10-μm diameter liposome comprised of the phospholipid 15-OPC. λ_G and λ_L correspond to the peak emission wavelengths for the gel and liquid-crystalline states of the phospholipid bilayer, respectively.

be reliably measured. In principle, GP changes as small as 0.001 (0.1% error) can be measured, based on having a system S/N ratio of 10^3:1. In practice, however, fluctuations in fluorescence emission were found to produce GP variations of ±2% and ±15% for liposomes and CHO cells, respectively, for repeated measurements made on the same sample. Hence, the smallest GP change that that could be measured with the present system was 0.02. For a given sample population, intrasample variability was found to produce results having standard deviations of ± 5% (liposomes) and ± 20% (CHOs). When laser power fluctuations (±5%) and the accuracy of chamber temperature control (±0.025°C) are accounted for, the errors for the resultant $\Delta T/\Delta P$ ratio, as determined by the GP assay, were ±10% for liposomes and ±25% for CHO cells.

RESULTS AND DISCUSSION

The effects of optical trapping on sample heating were studied for two classes of samples, including organically engineered liposomes and CHO cells. These particular samples were chosen for study because they are comparable in size, shape, and composition; have bilayer membranes which undergo phase transitions and can be tagged with environmentally sensitive dyes probes; and can be easily confined by an optical tweezers. Both sets of samples were prepared first by incorporating the Laurdan dye into the cell membranes (Liu et al., 1994; Parasassi et al., 1990, 1991) in dye-to-phospholipid molar concentration ratios of between 1:10^2 and 1:10^3, and then placed in suspension in a PBS solution. Our experiments consisted of bringing a liposome or cell into the field-of-view of the microscope, exposing the cell to UV radiation, and then monitoring the GP. This process was performed before and after switching on the laser trapping beam and as functions of time and incident laser power. Time-gated excitation was used to prevent photobleaching of the membrane probes. In this case, a UV power density of <100 mW/cm^2 and an exposure time of 100 ms were used. Before optical trapping, the laser power and spot size of the focused IR beam were measured. For the CW Nd:YAG laser (λ = 1.064 μm), focused power levels were continuously varied from 0 to 500 mW. The focused spot size of the TEM_{00} laser mode was determined to be ~0.80 ± 0.15 μm at the sample plane using a scanning knife-edge when a 1.3 N.A. 100× microscope objective was used.

Before optical trapping, a GP plot was generated to serve as a calibration curve for sample temperature measurements. By slowly increasing the temperature of the sample chamber by means of a heating coil embedded within the upper microchamber, a set of fluorescence emission spectra as a function of temperature from a freely suspended liposome were acquired. This data was then converted into GP data (Fig. 5). For example, a liposome bilayer consisting of the phospholipid 15-OPC exhibits a phase transition temperature (T_t) of 31°C (Fig. 5). Below ~30°C, the bilayer is predominantly in the gel state, while above ~32°C, the bilayer is mostly liquid-crystalline in phase. Within the transition region, however, the slope of the GP curve is very steep, i.e. $\Delta GP/\Delta T$ = 0.39 ± 0.02/°C, and a large change in GP occurs for a very small change in temperature T. Hence, in the vicinity of T_t, the bilayer membrane and the GP figure-of-merit are the most sensitive to temperature variations. To make a measurement using the calibration curve (Fig. 5), the temperature of the liposome or cell is first preset to a value just below T_t by means of a heating coil embedded within the sample chamber. When the sample temperature is increased, for example, via the absorption of IR radiation from the trapping beam, the fluorescence of the sample undergoes a large red shift (>40 nm), thereby reducing the GP and providing a direct measure of ΔT. The spatial resolution of the measurement, and the region from which fluorescence is collected, is controlled by adjusting the size of an aperture located in the confocal microscope image plane.

The results of subjecting a 10-μm diameter 15-OPC liposome to trapping radiation at different power levels and exposure times were measured (Fig. 6). For the first 5 s of the experiment, the trapping laser beam was turned off, the liposome fluorescence was continuously excited in the UV, and the GP was held constant at a value of ~0.40, corresponding to an initial set point temperature of 30.5°C, a value

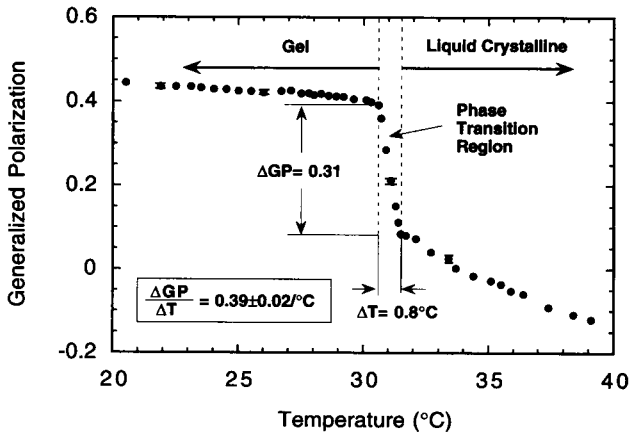

FIGURE 5 GP plotted as a function of liposome temperature. GP is derived from the fluorescence emission spectrum from a 10-μm diameter liposome measured by microfluorometry.

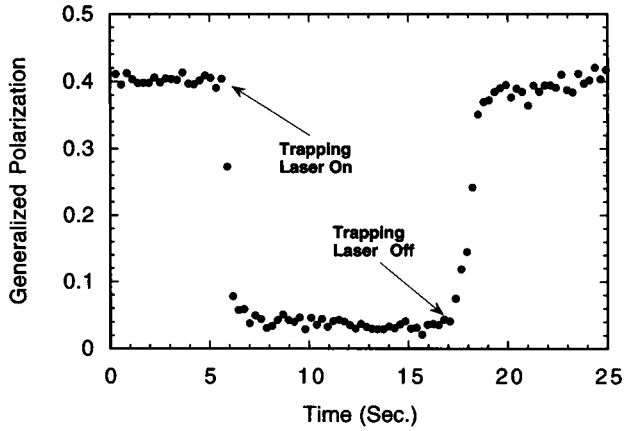

FIGURE 6 The change in GP as a function of time for a 10-μm diameter 15-OPC liposome first unconfined, and then confined, by a 170 mW infrared optical tweezers. The acquisition time for each data point is ~10 ms.

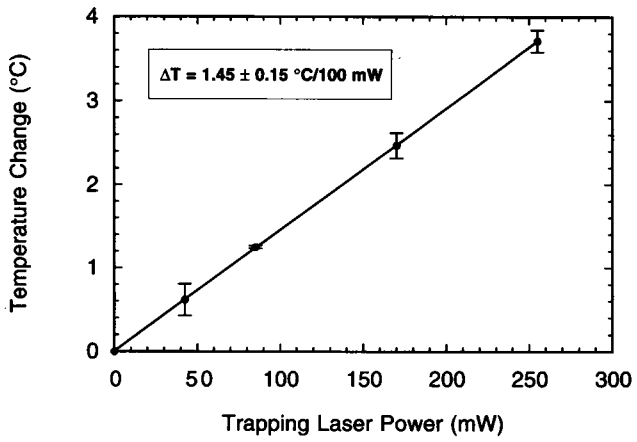

FIGURE 7 Relationship between induced temperature change and laser power of the incident IR trapping beam. Error bars represent the standard deviation for multiple measurements made at a given power level.

slightly below the transition temperature T_t of ~31°C. When the CW trapping laser (170 mW) was turned on, the liposome became trapped, and there was dramatic decrease in the value of GP to ~0.03, indicating a quick response to the applied laser trapping beam. Based upon the calibration curve (Fig. 5), a ΔGP of 0.37 between the initial and final states corresponds to a temperature increase of 2.4°C. For the next 10 s, as long as the trapping beam was kept on and used to confine the liposome, both the GP and sample temperature were held constant, and quasi-thermal-equilibrium conditions were established. However, as soon as the trapping beam was shut off, the liposome GP was observed to return back to its original value of 0.40, and the initial sample temperature was once again re-established. This clearly indicates that confinement by an IR trapping beam results in sample heating, as evidenced by a change in liposome bilayer membrane structure and a Stokes shift in the probe fluorescence spectrum. It also indicates that the phase transition process in the liposome is a reversible one, and that both the initial phase state and fluorescence emission spectrum can be recovered when the sample is cooled. The rise and fall times for the thermal switching process are estimated to be ~10 ms, respectively (Fig. 6), and are governed by the rate of heat conduction away from the locally heated region. When the trapping power was increased above 170 mW, a substantially larger change in GP and, hence, sample temperature, was observed. For example, at 255 mW, the liposome temperature was increased by nearly 3.7°C. By converting ΔGP data into ΔT values, the change in liposome temperature as a function of incident trapping power could be measured (Fig. 7). For Nd:YAG laser powers up to ~300 mW, the temperature is seen to be linearly proportional to the applied power, with liposomes exhibiting a heating rate of ~1.45 ± 0.15°C/100 mW.

The extent of cell heating induced by infrared optical tweezers can be understood in terms of a simplistic model that accounts for the power absorbed within a spherical region under laser irradiation (Appendix). The liposome absorption is assumed to be governed by that of water at the wavelength of 1.064 μm, rather than that of specific membrane or cell nucleus chromophores. In this case, the absorption coefficient for water is $\alpha \approx 0.1$ cm^{-1} (Katzir, 1993; Svoboda and Block, 1994). The results of calculations (Fig. 8) based on Eqs. 5 and 6 for a 10 μm diameter sample indicate that the initial heating rate at the position of the liposome membrane, located 5 μm away from the trapping beam focus, is very rapid (~10 ms), that a steady state condition is established within several hundred milliseconds of initial confinement by the IR tweezers, and that the final temperature change is linearly proportional to the incident laser power (P) and the water absorption coefficient (α). The general trends of transient and steady-state heating are the same for both the theoretical and experimental results (Fig. 8), and good agreement is obtained for the three laser powers of 85, 170, and 255 mW examined. The theoretical curves were completely determined by the use of fixed values for the water absorption coefficient, thermal conductivity of water, incident laser

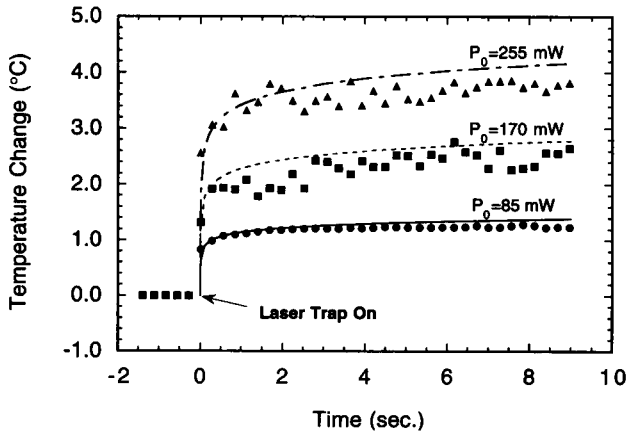

FIGURE 8 Transient temperature change plotted as a function of trap laser power and tweezers holding time. Experimental results for 85 mW (●), 170 mW (■), and 255 mW (▲) are compared with theoretically predicted values.

power, and sample size (radial distance from the beam focus). Small discrepancies between the measured and calculated values are likely to be due to several factors, including the use of an oversimplified heat conduction model that assumes an infinite water medium and neglects the finite boundaries imposed by the actual chamber geometry, the underestimation of the actual sample absorption coefficient, and the difference between the cell volumes which are irradiated by the IR trapping beam and sampled by the UV fluorescence excitation beam, respectively. However, based on the cell heating model (Appendix), both the initial temperature increase and the steady state equilibrium temperature can be predicted, based on knowing the sample radius (r), absorption coefficient (α), and incident laser power (P). As an example, a 2-μm diameter sample irradiated with 100 mW of IR trapping power would be expected to increase its temperature by 1.7°C within 1 s of laser exposure, and by 2.1°C after >10 s of laser irradiation.

Similar trapping experiments were also performed on living, nonmotile CHO cells. In comparison to the liposomes, which have a phospholipid bilayer membrane that can exist in one of two possible states, CHO cells have a more heterogeneous membrane structure and exhibit more subtle phase transition features, as assayed by the Laurdan probe and GP measurement technique. However, when Laurdan is incorporated into the cell membrane, it is still sensitive to the temperature and local environment of the membrane. The results of calibrated temperature measurements made on two different 10-μm diameter PBS-suspended spherical CHO cells (Fig. 9) show that the GP decreases in nearly a monotonic fashion with increasing temperature at a rate of $\Delta GP/\Delta T \approx 9.0 \pm 2.0 \times 10^{-3}$/°C. In comparison to the single-component liposome, CHO cells do not display a distinct phase transition feature at a given temperature in the GP curve. As a result, cellular GP measurements are less sensitive to small temperature variations, but display a greater linear dynamic range and can be used to quantify the extent of localized heating over a large temperature range. This GP broadening is probably due to the complex heterogeneous composition of cellular plasma membranes. It is interesting to note that some evidence for bilayer phase transition might be present at ~23.5, ~29, and 44°C in cell 1, and at ~27°C in cell 2, a behavior consistent with previously measured changes in the CHO plasma membrane fluidity (Dynlacht and Fox, 1992) that can give rise to distinct changes in the fluorescence and GP ratios. However, given the measurement errors, no definitive conclusions can be drawn about such transitions at this time. The differences in measured GP between the two cells examined (Fig. 9) are most likely derived from differences in physical membrane structure and the nonuniform incorporation of the Laurdan dye into the CHO membrane.

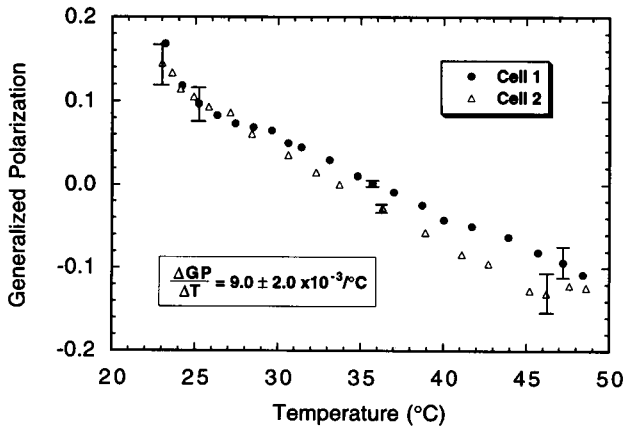

FIGURE 9 GP curve for two different CHO cells, cell 1 (●) and cell 2 (△), when the cells are heated from 23°C to 49°C.

As in the liposome samples, the shift in CHO fluorescence spectral response and decrease in GP is reversible when the cell temperature is decreased. With the application of a trapping laser beam, the CHO cell temperature was also observed to increase. For example, at 200 mW, the change in GP and temperature were 0.02 and 2.20°C, respectively. For multiple measurements (10 measurements per sample) made on five different CHO cells having approximately the same diameter, the average laser-induced temperature changes were found to vary between ~1.9 and 2.5°C, with a standard deviation of ~0.5°C. More specifically, for cells numbered 1 through 5, the means and standard deviations for measured values of ΔT (°C) were: 2.05 ± 0.44, 2.47 ± 0.49, 2.46 ± 0.46, 2.22 ± 0.49, and 1.90 ± 0.50, respectively. Similarly, over the range of laser powers examined, the CHO cells displayed a heating rate of ~1.15 ± 0.25°C/100 mW, a value very similar to that of the liposome samples. These variations may be due to intrasample variability arising during the culturing process, or the fact that the CHO cells may have a higher absorption coefficient due to their heterogeneous structure, or a thicker cell membrane wall that increases the optical absorption in the infrared.

The experimental and theoretical results presented above have shown that infrared optical tweezers induce cell heating and temperature increases of several degrees centigrade in liposomes and CHO cells for laser powers varying from tens to hundreds of milliwatts. Hence, for trapping powers of <100 mW, a ΔT of <1.0°C at 1.064 μm can be expected. Even larger temperature changes might be expected for other cell species having different absorption coefficients, or when the optical trapping process is performed at shorter wavelengths where chromophore absorption might be more significant. Thus far, it has been assumed that the infrared optical tweezers is purely noninvasive in nature. However, given the fact that the power densities considered herein are already on the order of 10^6–10^7 W/cm^2, values of ΔT of even a few degrees may be sufficient to affect the physiological state of the trapped cell. These factors may be of primary concern in, for example, the study of motile cells where several hundred milliwatts may be required to confine a cell in the trap. In the case of sperm cell trapping, temperature increases of several degrees have the potential to alter motility, impact fertilization capability, or cause damage to the genetic material contained within the sperm head. By contrast, in

chromosome and non-motile cell manipulation, where relatively small trapping powers are typically used (<100 mW), the present results suggest that direct thermal damage mechanisms may not be important for these samples. Of course, indirect effects, through processes such as gene activation and the generation of heat shock proteins (Marescan and Lindquist, 1990), may also play a role in the pathophysiology of optical traps. Some of these factors, particularly in motile cells, are presently under investigation. Hence, the present results should provide insight into the relative importance of thermal effects in optical trapping, provide new strategies for minimizing temperature increases, and allow users of optical tweezers to develop a better understanding of the techniques presented herein and their impact on cellular physiology and biology.

CONCLUSION

A novel and potentially powerful method for detecting minute temperature variations in optically trapped biological samples using Stokes-shifted fluorescence has been described. Temperature increases of several degrees centigrade have been directly measured for liposomes and CHO cells confined by a 1.064-μm optical tweezers. This work should form the basis for further studies into localized cell heating and the biological effects induced by the application of visible and near-infrared optical tweezers.

APPENDIX

The sample heating problem, defined by having a highly focused laser beam interact with a water-based absorbing particle immersed in a water bath, can be described by a diffusive partial differential equation of the form (Carslaw and Jaeger, 1959):

$$\nabla^2 T - \frac{1}{\kappa}\frac{\partial T}{\partial t} = -\frac{q}{K} \tag{1}$$

where T is the sample temperature, K is the thermal conductivity, κ is the thermal diffusivity constant, equal to $K/\rho c$ where ρ and c are the medium density and specific heat, and q is the energy absorbed per unit volume per unit time, respectively. To solve this equation, three basic approximations are made herein. First, given the fact that the core and membrane regions of the liposome and CHO cells are primarily water-based, having an absorption coefficient that is nearly identical to that of water (0.1 cm^{-1}) at the trapping wavelength of 1.064 μm, it is assumed that the heating contribution from the thin membrane regions (~5 nm) of the liposomes or cells can be neglected and that the medium to be heated is effectively an infinite homogeneous water medium. Second, we assume that the laser beam attenuation within a very small region of interest (<100 μm) can be neglected, owing to the relatively small magnitude of the absorption coefficient. Last, while the actual trapping process utilizes a focused Gaussian beam that is incident on the trapped sample at a beam convergence half-angle of ~60°, it is assumed for purposes of estimation that, within the infinite water bath, the incident laser beam uniformly irradiates a region over a half-angle of 90°, or a full convergence angle of 180°, i.e., that of a hemisphere.

Based on the above assumptions, the absorption rate q, or the release of heat at a given point in space and at a constant rate per unit time, can be written as:

$$q = q(r) = \frac{\alpha \cdot P}{2\pi r^2} \tag{2}$$

where α is the water absorption coefficient, P is the incident laser power, and r is the distance from the laser focus point. Eq. 2 indicates that the largest amount of heat is produced near $r = 0$, and decreases at the rate of $1/r^2$ away from the central region corresponding to the beam focus in the actual laser trap.

Eqs. 1 and 2 can be solved by recognizing this problem as that of a continuous spherical surface source (Carslaw and Jaeger, 1959), for which an integration sums up all the heating sources that are distributed throughout the entire water medium, and which contribute to heating at a particular point of interest. If heat is radiated at the rate $Q(t)$ per unit time over the surface of a sphere of radius r', starting at $t = 0$, then the temperature at a point r and time t is given by

$$\nu = \frac{1}{8\pi r r' (\pi\kappa)^{1/2}\rho c}\int_0^t \left\{\exp\left(-\frac{(r-r')^{1/2}}{4\kappa t}\right) - \exp\left(-\frac{(r+r')^{1/2}}{4\kappa t}\right)\right\}\frac{Q(t')dt'}{(t-t')^{1/2}} \tag{3}$$

where ρ is the density, c is the specific heat, and

$$Q(t') = 4\pi r^2 q = 2\alpha P \tag{4}$$

The integrand of Eq. 3 is the heat radiated from an instantaneous spherical surface source of radius r and unity strength at $t = 0$. Upon substitution and integration, Eq. 3 becomes

$$\nu = \frac{\alpha P}{4\pi\kappa\rho c r r'}\left\{2(\kappa t/\pi)^{1/2}\left[\exp\left(-\frac{(r-r')^{1/2}}{4\kappa t}\right) - \exp\left(-\frac{(r+r')^{1/2}}{4\kappa t}\right)\right] - |r-r'|\,\mathrm{erfc}\,\frac{|r-r'|}{2(\kappa t)^{1/2}} + (r+r')\,\mathrm{erfc}\,\frac{r+r'}{2(\kappa t)^{1/2}}\right\} \tag{5}$$

By integrating Eq. 5 for the continuous spherical surface heating sources ν over the entire medium, the temperature increase at a position r and for the time duration t of laser irradiation is given by:

$$T(r, t) = \int_0^\infty \nu dr' \tag{6}$$

For a given incident laser power power, P, and the physical constants of water (Weast et al., 1986) taken to be: $K = 0.597$ W/m°K, $\kappa = 1.43 \times 10^{-7}$ m^2/s, $\alpha = 10$ m^{-1}, $\rho = 10^3$ kg/m^3, and $c = 4182$ J/kg°K, Eqs. 5 and 6 can be solved for numerically, yielding the spatial and temporal temperature distribution $T(r, t)$ at position r and time t.

This work was supported by the National Science Foundation grant BIR-9121325 and National Institutes of Health grant R01-RR06961-01A2. D. K. Cheng acknowledges support under the NSF REU Program. Additional support was provided by resource grants from ONR (N00014-91-C-0134), DOE (DE-FG03-91ER61227), and an NIH LAMP grant R01-192 to the Beckman Laser Institute and Medical Clinic.

REFERENCES

Ashkin, A., and J. M. Dziedzic. 1987. Optical trapping and manipulation of viruses and bacteria. *Science*. 235:1517–1520.

Ashkin, A., and J. M. Dziedzic. 1989. Internal cell manipulation using infrared laser traps. *Proc. Natl. Acad. Sci. USA*. 86:7914–7918.

Ashkin, A., J. M. Dziedzic, J. E. Bjorkholm, and S. Chu. 1986. Observation of a single-beam gradient force optical trap for dielectric particles. *Opt. Lett.* 11:288–290.

Ashkin, A., J. M. Dziedzic, and T. M. Yamane. 1987. Optical trapping and manipulation of single cells using infrared laser beams. *Nature*. 330: 769–771.

Berns, M. W., W. H. Wright, B. J. Tromberg, G. A. Profeta, J. J. Andrews, and R. J. Walter. 1989. Use of a laser-induced optical force trap to study chromosome movement on the mitotic spindle. *Proc. Natl. Acad. Sci. USA*. 86:4539–4543.

Block, S. M., L. S. B. Goldstein, and B. J. Schnapp. 1990. Bead movement by single kinesin molecules studied with optical tweezers. *Nature*. 348: 348–352.

Carslaw, H. S., and J. C. Jaeger. 1959. Conduction of Heat in Solids. Oxford University Press, Oxford, UK. 261–263.

Colon, J. M., P. Sarosi, P. G. McGovern, A. Ashkin, J. M. Dziedzic, J. Skurnik, G. Weiss, and E. M. Bonder. 1992. Controlled micromanipulation of human sperm in three dimensions with an infrared laser optical trap: effect on sperm velocity. *Fertil. Steril.* 57:695–698.

Dynlacht, J. R., and M. H. Fox. 1992. Heat-induced changes in the membrane fluidity of Chinese hamster ovary cells measured by flow cytometry. *Rad. Res.* 130:48–54.

Finer, J. T., R. M. Simmons, and J. A. Spudlich. 1994. Single myosin molecule mechanics: piconewton forces and nanometre steps. *Nature*. 368: 113–119.

Firester, A. H., M. E. Heller, and P. Sheng. 1977. Knife-edge scanning measurements of subwavelength focused light beams. *Appl. Opt.* 16:1971–1974.

Freshney, R. I. 1987. Culture of Animal Cells. Wiley-Liss, New York. 397.

Katzir, A. 1993. Lasers and Optical Fibers in Medicine. Academic Press, San Diego. 76.

Kuo, S. C., and M. P. Sheetz. 1992. Optical tweezers in cell biology. *Trends Cell Biol.* 2:116–234

Kuo, S. C., and M. P. Sheetz. 1993. Force of single kinesin molecules measured with optical tweezers. *Science*. 260:232–234.

Liang, H., W. H. Wright, C. L. Rieder, E. D. Salmon, G. Profeta, J. Andrews, Y. Liu, G. J. Sonek, and M. W. Berns. 1994. Directed movement of chromosome arms and fragments in mitotic newt lung cells using optical scissors and optical tweezers. *Exp. Cell Res.* 213:308–312.

Liu, Y., D. K. Cheng, G. J. Sonek, M. W. Berns, and B. J. Tromberg. 1994. A microfluorometric technique for the determination of localized heating in organic particles. *Appl. Phys. Lett.* 65:919–921.

Marescan, B., and S. Lindquist, editors. 1990. Heat Shock. Springer-Verlag, Berlin.

Misawa, H., M. Koshioka, K. Sasaki, N. Kitamura, and H. Masuhara. 1991. Three-dimensional optical trapping and laser ablation of a single polymer latex particle in water. *J. Appl. Phys.* 70:3829–3836.

Oku, N., J. F. Scheerer, and R. C. MacDonald. 1982. Preparation of giant liposomes. *Biochim. Biophys. Acta*. 692:384–389.

Parasassi, T., G. DeStasio, A. d'Ubaldo, and E. Gratton. 1990. Phase fluctuation in phospholipid membranes revealed by Laurdan fluorescence. *Biophys. J.* 57:1179–1186.

Parasassi, T., G. DeStasio, G. Ravagnan, R. M. Rusch, and E. Gratton. 1991. Quantitation of lipid phases in phospholipid vesicles by the generalized polarization of laurdan fluorescence. *Biophys. J.* 60:179–189.

Perkins, T. T. S. R. Quate, D. E. Smith, and S. Chu. 1994. Relaxation of single DNA molecule observed by optical microscopy. *Science*. 264: 822–826.

Perkins, T. T., D. E. Smith, and S. Chu. 1994. Direct observation of tube-like motion of a single polymer chain. *Science*. 264:819–822.

Schutze, K., and A. Clement-Sengewald. 1994. Catch and move—cut or fuse. *Nature*. 368:667–669.

Schutze, K., A. Clement-Sengewald, and A. Ashkin. 1994. Zona drilling and sperm insertion with combined laser microbeam and optical tweezers. *Fertil. Steril.* 61:783–786.

Svoboda, K., and S. M. Block. 1994. Biological applications of optical forces. *Annu. Rev. Biophys. Biomol. Struct.* 23:247–285.

Svoboda, K., C. F. Schmidt, B. J. Schnapp, and S. M. Block. 1993. Direct observation of kinesin stepping by optical trapping interferometry. *Nature*. 365:721–727.

Tadir, Y., W. H. Wright, O. Vafa, T. Ord, R. H. Asch, and M. W. Berns. 1989. Micromanipulation of sperm by a laser generated optical trap. *Fertil. Steril.* 52:870–873.

Vorobjev, I. A., H. Liang, W. H. Wright, and M. W. Berns. 1993. Optical trapping for chromosome manipulation: a wavelength dependence of induced chromosome bridges. *Biophys. J.* 64:533–538.

Weast, R. C., M. J. Astle, and W. H. Beyer, editors. 1986. Handbook of Chemistry and Physics, 67th ed. CRC Press, Boca Raton, FL.

Wright, W. H., G. J. Sonek, and M. W. Berns. 1994. Parametric study of the forces on microspheres held by optical tweezers. *Appl. Opt.* 33:1735–1748.

Yatvin, M. B., I. M. Tegmo-Larsson, and W. H. Dennis. 1987. Temperature- and pH-sensitive liposomes for drug targeting. *In* Drug and Enzyme Targeting. R. Green and K. J. Widder, editors. Academic Press, New York. 77–87.